Modification of Electronic Structure of Cs_2TCNQ_3 with Magnetic Field

Hasanudin[1]*, Noritaka Kuroda[1], Toyonari Sugimoto[2], Masayuki Hagiwara[3], Kazumasa Ueda[2], Toshiji Tada[2], Hiroshi Uozaki[4], Naoki Toyota[4], Iwao Mogi[5], Kazuo Watanabe[5]

[1]Department of Mechanical Engineering and Materials Science, Faculty of Engineering Kumamoto University, Kumamoto 860-0855, Japan
[2]Research Institute for Advanced Science and Technology, Osaka Prefecture University, Sakai 599-8570, Japan
[3]Institute of Physical and Chemical Research (RIKEN), Wako 351-0198, Japan
[4]Department of Physics, Graduate School of Science, Tohoku University, Sendai 980-8577, Japan
[5]Institute for Materials Research, Tohoku University, Sendai 980-8577, Japan

Abstract

The crystals of the organic semiconductor Cs_2TCNQ_3 have been successfully grown under strong external magnetic field, and their properties are compared with those of the crystals grown without magnetic field. The crystals grown under magnetic field higher than a certain temperature-dependent threshold field show remarkable change in electric, magnetic, and optical properties, despite no significant change in the crystal morphology and structure. Electric conductance data suggest the increasing of acceptors in the crystals grown under magnetic field, which is accompanied by the increasing of the Curie temperature by the amount of 100 K, and the intensification of the absorption band arises from inter-radical charge transfer transition. These results suggest that some newly electronic states have been induced by the applied field during the crystal growth.

1. Introduction

High magnetic field has been widely used to manipulate the properties of materials by applying it in the course of chemical reaction and crystal growth. The electromagnetic forces, for example, function to align fibrils of biomolecules[1,2] or control the nucleation rate, size and orientation of crystalline proteins[3] and organic molecules[4]. Similar effects have been confirmed to take place on the nucleation and orientation of grains of metallic alloys. In recent years, therefore, there have been extensive studies on the application of high magnetic field for synthesizing films and tapes of high T_c superconductors from vapor phase[5].

The present work deals with a strongly-correlated organic semiconductor system, Cs_2TCNQ_3, a prototype of TCNQ (tetracyanoquinodimethane) complexes with neutral/radical molecules ratio of 1:2. This ratio means that in the crystal structure there exists both radical and neutral TCNQ

---

* Visiting Researcher invited with the 100th Anniversary Foundation, Faculty of Engineering, Kumamoto University

molecules. Cs_2TCNQ_3 is crystallized from solution and applying external magnetic field to this solution will give the Lorentz force selectively on the radical molecules as well as Cs^+ ions, which are charged, and causes cyclotron motion of those ions/molecules. In the interface of solution-solid states, this motion will raise the perturbation to the chemical potential, which will possibly lead to a remarkable change in the crystal structure, and therefore in their other properties. Thus, it is very interesting to explore the effect of the Lorentz force applied during the crystal growth to the properties of the obtained crystals. We have grown the crystals of this complex under strong magnetic field to explore the effect of the applied magnetic field during the crystal growth to their morphology, orientation, as well as the electronic structure.

Another factor has to be considered in this experiment. In addition to the Lorentz force, the molecules are also under the influence of thermodynamic forces. These forces contribute to the movement of the molecules as well. At high temperature, the thermodynamic forces might be comparable to the Lorentz force. If the above-mentioned Lorentz force affects the properties of the obtained crystals, it is then also very important to explore how temperature affects these effects.

Cs_2TCNQ_3 is reported to exhibit a ferromagnetic behavior with extremely small saturated moment, and this ferromagnetism remains even at room temperature[6]. The widely known mechanisms such as RKKY are not suitable to explain this novel behavior. Ueda *et al.*[6] have suggested the spin canting due to the Dzyaloshinsky-Moriya interaction as the origin. However, such interaction is not possible to exist in the system with center of inversion like the case of Cs_2TCNQ_3. This ferromagnetism, therefore, must arise from unusual origins, which unfortunately remain unknown to the date.

The present substance is crystallized into a monoclinic structure in which the Cs^+ ions and TCNQ molecules are stacked along the b axis. The stack itself is made of radical (A) and neutral (B) molecules, which are aligned as the repetition of BAABAAB..... The distances of AA and AB are 3.26 and 3.22 Å, respectively[7]. The electrons provided by the donors, Cs atoms, are not homogeneously distributed over the TCNQ column, but are localized on the $TCNQ^-$ molecules[8]. Such distribution is achieved because the Coulomb repulsion energy of the π^* electrons, U~1.2 eV, is much larger compared to the transfer integral t~0.3 eV[9]. This system is, therefore, can be regarded as the 1/3-filled Pierls-Hubbard system[10]. In the ground state the π^* electrons of the radical molecules are in the singlet state and the energy to the triplet state $4t^2/U$ is found experimentally to be ~0.12 eV[11].

Lattice imperfection is one of the most important issues in semiconductors research. In many cases, lattice imperfections can act as donors and acceptors to give raise to the electric conductivity, as well as to change the optical properties of the normally insulating materials. Similar case is also found in Cs_2TCNQ_3. Based on the electrical conductivity measurement by Blackmore *et al.*[12], Cs_2TCNQ_3 is found to have a thermally excited energy gap of $E_G = 0.6$ eV and the p-type conductivity carrier is conducted by the acceptors with density of $\sim 1 \times 10^{17}$ cm^{-3}. The origins as well as the other roles of these acceptors, however, have never been properly explored. It is our interest to examine their relation to the magnetic properties of this substance.

Optical measurement can provide valuable information regarding these matters. Impurities, lattice disorders, etc., can be observed very well through the optical forbidden rules accompanying the lowering of the symmetries. Optical properties of Cs_2TCNQ_3 actually, have been previously explored by several authors[13,14]. However, most of these works discussed their results in term of general view of the electronic structure of TCNQ complexes. The importance of the impurities, for example, has never been properly explored.

A pressure-induced electronic transition, which resembles to the insulator-metal transition, has been observed from the electrical resistivity measurement in the present substance[15]. This metal-like state, however, is different from that of ordinary metals, since no Drude tail is observed in the high-pressure phase of its infrared absorption spectrum[16]. High-pressure Raman scattering as well as infrared absorption studies have shown that π^* electrons of the $TCNQ^-$ are significantly delocalized in the high-pressure phase[17,18]. The delocalization, however, is not complete so that the above-mentioned localization character is maintained, and therefore the substance maintains its semiconducting character. In addition, the infrared absorption data have also suggested that this phase transition is accompanied by a symmetry change in the relative position of the $TCNQ^-$ radical molecules. In the low-pressure phase they are displaced against each other along the short molecular axis forming slipped dimers, whereas in the high-pressure phase those dimers turn into eclipsed ones[17].

The purpose of the present work is to examine the possibility of using the Lorentz force mentioned above for manipulating the electronic structure as well as the properties of a substance. It is also our purpose to investigate the conditions required for obtaining such effects. In addition, the properties of the perturbed system, i. e. the crystals grown under magnetic field, can be expected to reflect the properties of the original system. In this sense, this method can also be used to understand the unusual ferromagnetism in this substance. For these purposes, we have grown the crystals of this substance under strong magnetic field and examined the crystal structure, as well as measured their temperature dependence of electric resistivity, magnetization, and optical absorption of the obtained crystals. The results are compared to the properties of the crystals grown without magnetic field.

The above-mentioned pressure-induced phase transition provides a good chance to explore the differences between the two crystals. The change in the electronic structure can be expected to change the properties of the crystal under high pressure. To explore this point, we also have measured the high-pressure infrared absorption in the 5 T crystals and compared the results with the same experiment on 0 T crystals.

2. Experimental procedure

The crystals are grown by a standard mixed-solvent method. The nearly saturated acetonitrile solution of Cs_2TCNQ_3 is prepared in a glass bottle. The bottle is encapsulated in a larger bottle together with diethyl ether, while the inner bottle being kept open. This dual container system is settled on the central position of the magnetic field of a cryogen-free superconducting magnet, which can generate magnetic field up to 11 T. The temperature of the system is regulated at 10 and 20 ℃. As the vapor of diethyl ether recondenses to mix with the solution, the Cs_2TCNQ_3 crystals precipitate as small needles and thin platelets. After a few days a half amount of the dissolved material crystallizes.

The morphology of the obtained crystals is observed under optical microscope with magnification of 20 times. Four-axes X-ray diffraction has been employed to analyze the crystal structure. The temperature dependence of the electrical resistivity is measured using the four-probes method in the temperature range of 70-400 K. The magnetic moment as well as its temperature dependence is measured using SQUID.

The as grown single crystals, approximately 100x150 μm^2 wide, and 10 μm thick, are used as the samples during the optical measurements. The wide surfaces of the samples are parallel to the ab plane of the crystals, and the probe light incident normal to these surfaces. For optical absorption

measurement in the ambient pressure, the samples are placed in the temperature-controllable optical cell, with temperature range of 90 - 450 K. A diamond anvil cell (DAC) is used to generate pressure for measuring the infrared absorption under high pressure. Daphne oil and flourinert are complementarily employed as the pressure-transmitting medium, depending on the spectral region being observed, due to the problem explained previously[17]. The infrared absorption is measured using an FT-IR spectrometer equipped with a microscope. The ruby florescence method is used for calibrating the pressure.

3. Results

3.1. Crystal morphology and structure

Regardless the strength of the applied field, the crystals grown under magnetic field are the mix of needle and plate types, similar to that usually found when they are grown without magnetic field. They are grown in a random order on the wall and base of the bottle. The observation under a optical microscope with magnification up to 20 times cannot distinguish the crystals grown under magnetic field from those grown without magnetic field. In addition, the four-axes X-ray diffraction has been performed to analyze the crystal structure. Within the range of experimental error, there is no significant difference in crystal orientation as well as lattice constants compared to the crystals grown without magnetic field.

3.2. Electric properties

Figure 1 shows the temperature dependence of electric conductance in the crystals grown under 0 and 5 T (hereafter will be denoted as 0 and 5 T crystals, respectively). Because the size of the crystals is very small, the size of the samples as well as the probe distance cannot be precisely estimated, so that the experimental data cannot be converted to conductivity. The value of the conductance multiplied by a factor 1×10^2 gives an estimation of the conductivity in the units of S/cm. The behavior of the 0 T crystals agrees very well with the previous observation by Blakemore *et al.*[12]. At low temperatures the electric carriers, being holes according to the detailed study of Blakemore

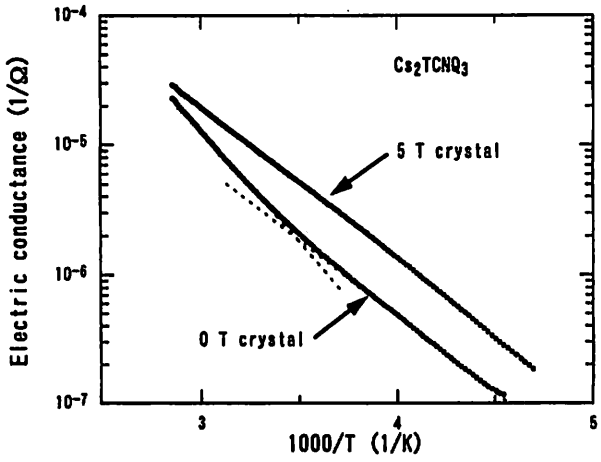

Figure 1. Temperature dependence of electric conductance in 0 T and 5 T crystals.

et al., are thermally produced with activation energy of 0.24 eV. At around 290 K, the thermal excitation of the carriers changes to obey the activation energy of 0.36 eV at high temperatures. The 5 T crystals, on the other hand, exhibit the conductance greater than that of 0 T crystals in the whole temperature range of the present measurement. In addition, the activation energy is independent of temperature up to 350 K. It is evident that the acceptor concentration of 5 T crystals is significantly higher than Blakemore's value 1×10^{17} cm^{-1} of the 0 T crystals.

3.3. Magnetic properties

Figure 2(a) and 2(b) show the magnetization curves of the 5 T crystals at 300 K and 400 K, respectively, where the inherent diamagnetic moment, -8.27×10^{-5} emu/G/mol, of TCNQ molecules is subtracted from the original data. At 300 K one may identify a weak but clear hysterisis loop of ferromagnetic magnetization on a small paramagnetic background. A similar ferromagnetic behavior has also been observed in 0 T crystals at room temperature[6]. The coercive force is ~100 G for both crystals. If temperature is raised to 400 K, the ferromagnetic component is reduced largely, while the paramagnetic background is enhanced. The paramagnetic moment is known to arise from thermally excited triplet spin state[11] lying at 0.12 eV above the singlet ground state mentioned at the beginning.

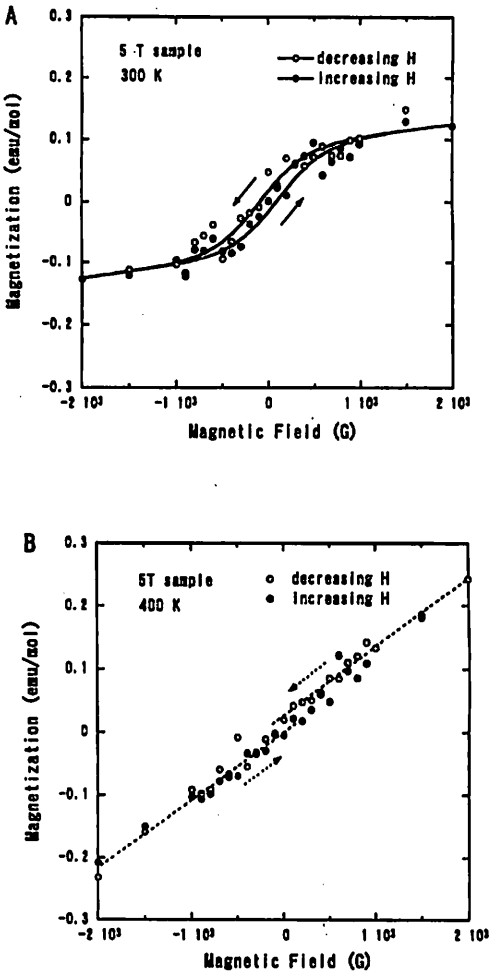

Figure 2. Magnetization curve of 5 T crystals at (a) 300 K and (b) 400 K.

To see the temperature dependence of the ferromagnetic behavior we have measured the magnetization at a fixed magnetic field of 1 x 10^3 G in a wide range of temperature in both crystals. The results are subtracted from the contributions from the Curie-law impurities, being significant at low temperatures, and the thermally excited triplet spin state as well as the inherent diamagnetism of TCNQ molecules, to extract the ferromagnetic moment. The ferromagnetic component of the magnetization after subtraction as the function of temperature are shown in Fig. 3 for 0 T and 5 T crystals. In the 0 T crystals the moment tends to collapse around 320 K, whereas it perseveres up to about 400 K in the 5 T crystals, in consistence with the magnetization curves shown in Fig. 2(b).

3.4. Optical properties

3.4.1. Intergap and intragap electronic transition

Figure 4 (a) and (b) show the linearly polarized optical absorption spectra in the region near the

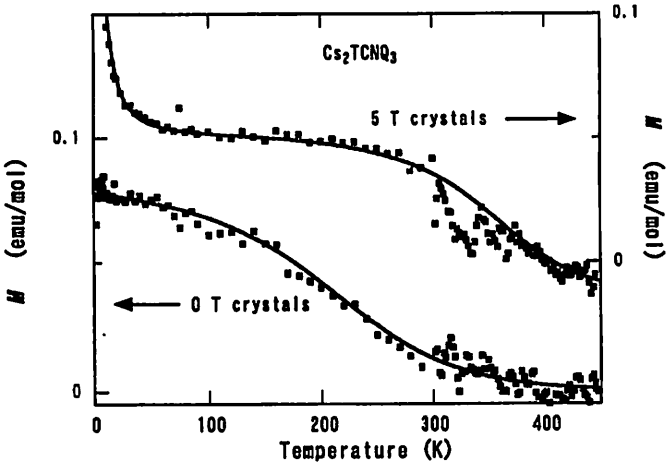

Figure 3. Temperature dependence of ferromagnetic component of magnetization in 0 T and 5 T crystals.

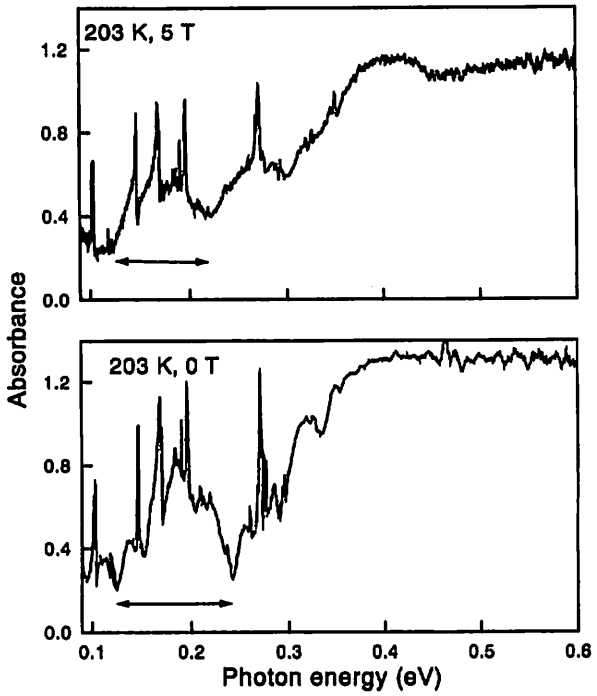

Figure 4. Linearly polarized optical absorption spectra in the mid-infrared region in (a) 0 T and (b) 5T crystals.

fundamental absorption in 0 and 5 T crystals, respectively. For both crystals, we can observed several sharp peaks appear in the region below 0.3 eV arise from molecular vibrations. At higher energy there appears a broad absorption band arises from 0.3 eV with the center at around 0.6 eV in the E//b polarization. Similar band, however, does not appear for E//a polarization. This band can be assigned to the electronic transition from the π^* orbitals of radical molecules to that of the neutral molecules, which equivalent to the interband transition. The step shape of the absorption edge suggests that the gap is a direct type, which is in good agreement with Soos and Klein[10] proposal based on the modified Hubbard model.

Inside the gap, in both 0 and 5 T crystals, in the spectral region from 0.015 to 0.3 eV there appears several absorption bands, which are suggested to arise from band-to-bound levels in the gap. We would stress here that those band-to-bound electronic bands can be observed only for the *E//b* polarization. If we take a careful look to these bound states, we will notice that in 5 T crystals there appears an additional weak structure at ~0.4 eV. Such structure does not appear in 0 T crystals. In addition, the structure appears at around 0.18 and 0.28 eV shifted to the lower energy side by amount of 0.01 eV, and their intensities are slightly enhanced in 5 T crystals.

3.4.2. Inter-Hubbard level transition

The linearly polarized optical absorption spectra in the energy region higher than 1 eV are shown in Fig.5 for both 0 T and 5 T crystals. In E//b polarization there is no significant difference between 0 and 5 T crystals. There appears a strong and broad band denoted as B in the energy region of 1-2 eV. This band has been previously assigned to the electronic transition from lower to upper Hubbard levels of the valence band[11,12]. This transition can be simply understood as the charge transfer from between the two adjacent radical molecules. In the E//a polarization, on the other hand, the absorption band arises from the $\pi-\pi^*$ localized excitation in the radical molecules, which is denoted as C band, appears at 2.2 eV. Because it is almost forbidden in E//a polarization, the above-mentioned inter-radical charge transfer manifest itself as a weak band, which is denoted as S1, in 0 T crystals. However this band is remarkably intensified in 5 T crystals. The S1 band in both crystals diminishes with increasing temperature. In 0 T crystals, it already becomes barely

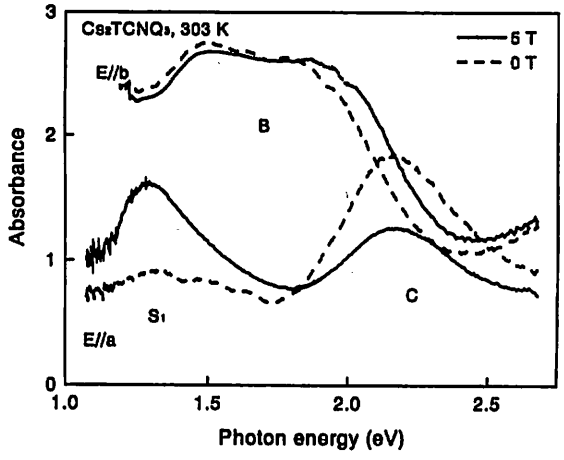

Figure 5. Linearly polarized optical absorption spectra in the near-infrared to visible region in 0 T and 5T crystals.

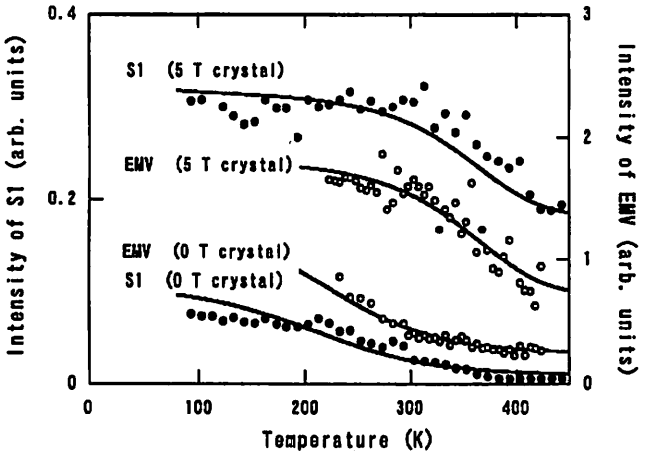

Figure 6. Temperature dependence of integrated intensity of S1 band as well as EMV mode at 1360 cm-1 in 0 T and 5 T crystals.

observable at around 400 K. In 5 T crystals, on the other hand, remains quite intense at the same temperature. The temperature dependence of the integrated intensity of S1 band normalized with that of C band in both crystals, which are shown in Fig. 6 clearly show this difference.

3.4.3. Molecular vibration

The overall molecular vibration features are very similar in both crystals. As very well known, infrared absorption spectrum appears as the superposition of the antisymmetric vibration modes belonging to the $TCNQ^0$ and $TCNQ^-$, as the consequence of the aforementioned localization scheme[8]. The frequencies of those vibrations are the same in both crystals. In addition those vibration modes, the infrared properties of this substance are featured with the totally symmetric

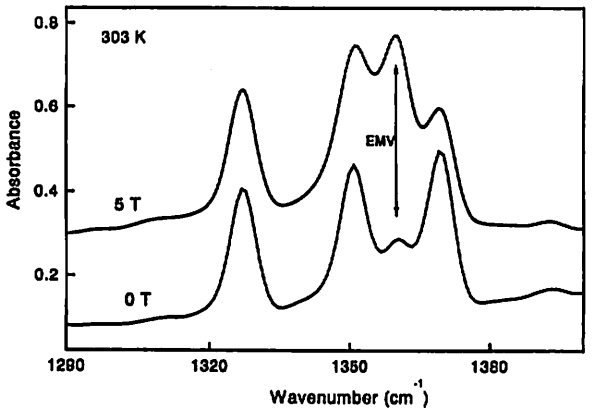

Figure 7. Infrared absorption spectrum due to the molecular vibration in the C-H bending region for 0T and 5T crystals.

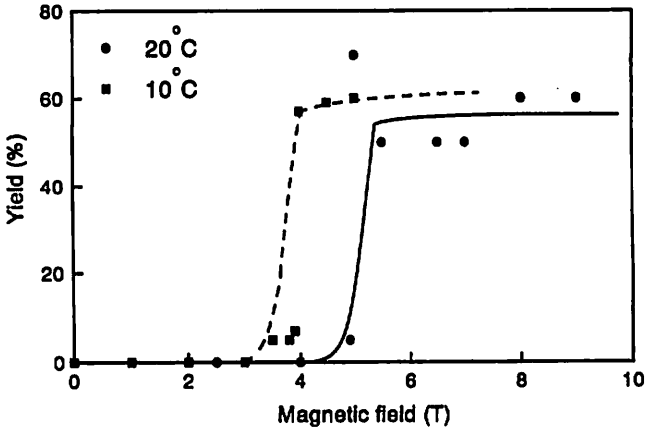

Figure 8. Field dependence of the yield of the crystals with the magnetic field effect.

modes, which become infrared active by the electron-molecular-vibration (EMV) interaction with the inter-Hubbard level transition mentioned in the previous section. Their properties in E//b polarization have been studied both experimentally and theoretically[8,9], and no significant difference is observed for the vibration modes in this polarization.

We particularly pay attention on the EMV modes observed in E//a polarization, where they are originally forbidden. Figure 7 shows the infrared absorption in the C-H bending region, as an example. In 0 T crystals the EMV mode appear at 1360 cm^{-1} with very weak intensity so that it is barely observable even at low temperature. In 5 T crystals it also appear at the same energy, but with enhanced intensity, so that it becomes comparable to normally infrared active modes. We believe that this enhancement is the effect of the applied field during the crystals growth, as similarly happened to the S1 band. We have also measured the temperature dependence of the intensity of EMV mode, and it emerges that the intensity of this mode in respective crystals has similar temperature dependence with S1 band as shown in Fig.6. Several other EMV modes also show similar properties.

3.4.4. Field and temperature dependence

The effects of magnetic field explained above do not appear in all crystals grown under magnetic field. Based on the infrared properties, we found that the crystals with the magnetic field effect can only be obtained if they are grown under the magnetic field stronger than a certain threshold value. Figure 8 shows yield of the crystals with magnetic effect as the function of the applied field. As clearly seen in Fig. 8, for the crystals grown at 20℃ the threshold is 5 T, whereas for those grown at 10℃ the threshold is 4 T. Below these threshold values, the yield is almost zero percent. The yield is abruptly increases to about 60% when the field is stronger than the thresholds, and this value is maintained at the field stronger than the threshold.

3.5. Infrared absorption under high pressure

Figure 9 (a) and (b) show the unpolarized infrared absorption in the C-CN stretching region in 5 T and 0 T crystals, respectively, at several pressures. Figure 9 (b) is taken from ref. 17 for

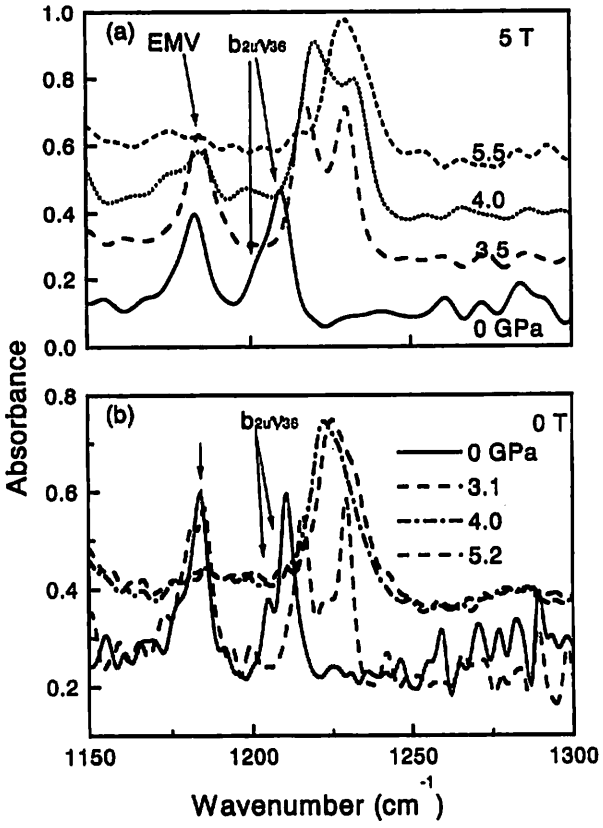

Figure 9. Absorption spectra in the C-CN stretching region at several pressures.

comparison. The thickness of the samples is ~10 μm. The features observed at 1205 and 1211 cm^{-1} at the ambient pressure are the infrared active $b_{2u}(\nu_{36})$ modes belonging to the neutral and radical molecules, respectively, whereas the one at 1184 cm^{-1} is the electron-molecular vibration (EMV) coupled mode[16,17]. At low pressures, the two $b_{2u}(\nu_{36})$ modes behaves similarly in 0 T and 5 T crystals; they exhibit a blue-shift with increasing pressure, while increasing their frequency spacing. In 0 T crystals, at around 3.6 GPa they abruptly shorten their frequency spacing to appear like a broad single line. Above 3.6 GPa they keep blue-shifting without changing their frequency spacing. Similar behavior is observed in 5 T crystals as well, but the frequency spacing gets shortened at higher pressure than that in 0 T crystals. Figure 9 (a) clearly shows a splitting of the $b_{2u}(\nu_{36})$ modes belonging to the neutral and radical molecules at 4.0 GPa in 5 T crystals, which is in contrast to that in 0 T crystals where they already appear as a broad single line at about the same pressure. The difference can be observed more clearly from the pressure dependence of frequencies of those vibration modes shown in Fig. 10. It is clear from the figure that the behavior of the both crystals, is very similar in the low-pressures but is different at high-pressures.

Significant differences can also be observed from the behavior of the EMV coupled mode observed at 1184 cm^{-1}. As clearly seen in Fig. 9 (a) and (b), the most distinct difference lies on the fact that EMV mode remains observable at pressures higher than 3.6 GPa, in contrast to the 0 T crystals in

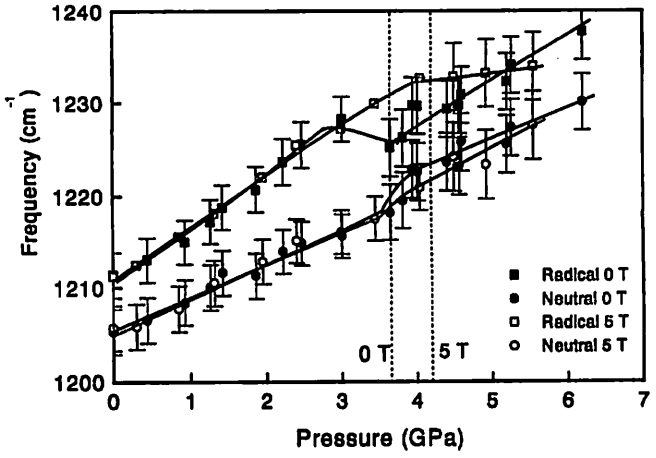

Figure 10. Pressure dependence of the frequency of the C-CN stretching in 0 T and 5 T crystals. The error bars represent the width of the absorption bands, and the vertical dotted lines in the graph indicate the transition points in respective crystals.

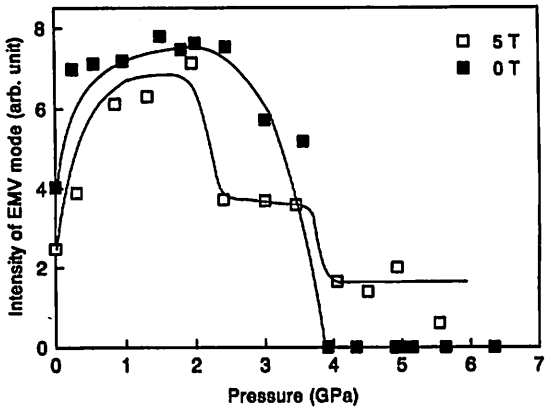

Figure 11. Pressure dependence of the integrated intensity of EMV mode observed at 1184 cm^{-1} at ambient pressure in 0T and 5 T crystals.

which the EMV coupled mode disappears. If we compare the spectrum at 4 GPa in both crystals we can clearly notice that in 5 T crystals the EMV coupled mode remains, whereas it is already disappear at the same pressure in 0 T crystals. The pressure dependence of the intensity of EMV band in both crystals displayed in Fig. 11 shows the difference more clearly. The EMV mode in 0 T crystals gradually intensified with increasing pressure up to 3.0 GPa, and abruptly diminishes at higher pressure 3.6 GPa. In 5 T crystals, on the other hand, the same band is gradually intensified as pressure increases up to 2 GPa, and abruptly decreases in some steps, to be barely observable at pressures higher than 5.5 GPa. This behavior is very similar to the pressure dependence of S1 band,

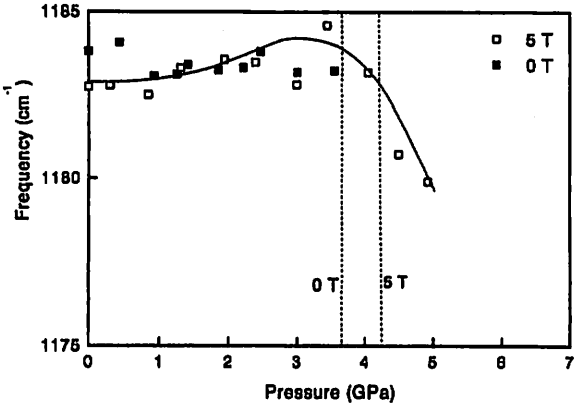

Figure 12. Pressure dependence of the frequency of EMV mode observed at in 0T and 5 T crystals.

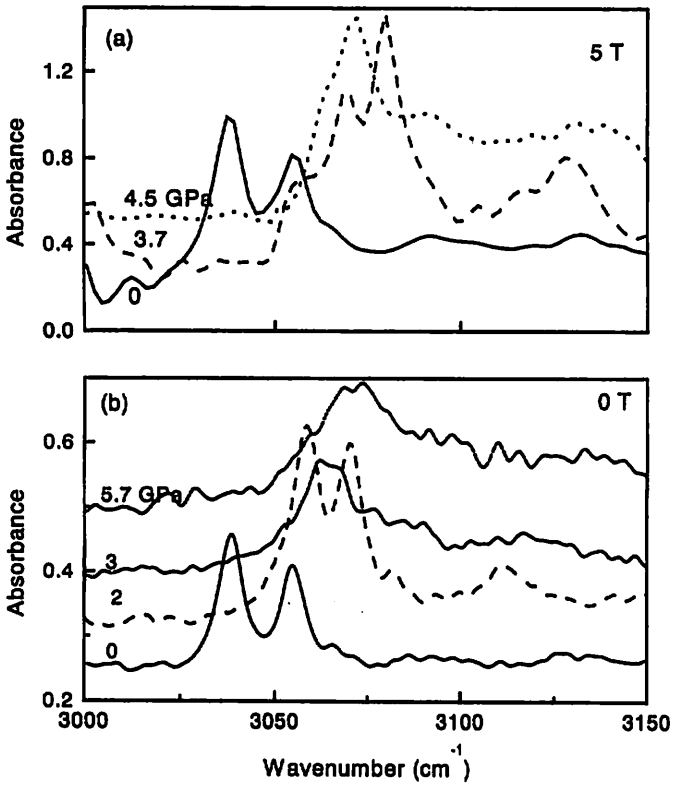

Figure 13. Pressure dependence of the frequency of the C-H stretching in 0 T and 5 T crystals.

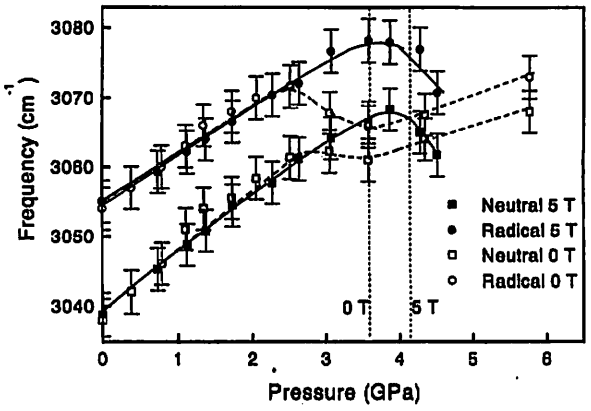

Figure 14.

the coupling counterpart of the EMV modes[18,19]. The pressure dependence of the frequency of the above-mentioned EMV mode in 5 T crystals is plotted together with that of 0 T crystals, and is shown in Fig. 12. It emerges from the figure that the EMV mode in the high-pressure phase of the 5 T crystals exhibits a red-shift with increasing pressure.

Figure 13 (a) and (b) show the infrared absorption spectrum in the C-H stretching region at several pressures in 5 T and 0 T crystals, respectively. The two modes appear at 3038 and 3054 cm^{-1} at ambient pressure are the b modes belonging to the neutral and radical molecules, respectively. The pressure dependence of these modes in both crystals are shown in Fig. 14. In both crystals at low pressures they are blue-shifted with increasing pressure while gradually reducing their frequency spacing. In 0 T crystals at ~3.0 GPa these modes shift toward lower frequencies while abruptly reducing their frequency spacing. They recover blue-shifting while maintaining their frequency spacing at pressure higher than 3.6 GPa. In 5 T crystals those mode tend to exhibit similar behavior, where they start to shift toward lower frequencies while reducing their frequency spacing at 4.1 GPa. The observation at pressures higher than 5.5 GPa, however, is difficult, since the C-H vibration modes become barely observable for the unclear reasons.

4. Discussion

The optical properties of the crystals grown even in the magnetic field stronger than the threshold do not show any significant difference from those of the crystals grown without field, except in several points mentioned above. The B and C bands, as well as the normally infrared active vibration modes, for example, remain unchanged. This means that the electronic structure basically does not change, which in good agreement with the fact that the crystals structure studied by the X ray diffraction analyses does not show any significant difference either.

This properties of S1 band and EMV modes in the 0 T crystals of Cs_2TCNQ_3 reminiscent of similar band in $(NMe_4)_2TCNQ_3$[18,19]. The S1 band and EMV modes of $(NMe_4)_2TCNQ_3$ disappear at around 338 K following the structural phase transition in which the slipped dimers at low-temperature phase transform into perfectly eclipsed dimers at higher temperatures[18-20]. We have assigned the S1 band in $(NMe_4)_2TCNQ_3$ to the a-axis component of the inter-radical charge transfer transition band. This band is supposed to be polarized along b-axis, but its dipole moment has a

weak component along a-axis because the $TCNQ^-$ molecules are stacked in a slipped fashion[6]. The $TCNQ^-$ molecules in the present substance are also stacked in similar fashion, so we assign the S1 band in the present substance similarly to that of $(NMe_4)_2TCNQ_3$. The S1 band in Cs_2TCNQ_3, however, remains until the sample decomposed at around 473 K, suggesting that similar phase transition does not occur.

Interestingly, despite the resemblance properties of S1 band in both substances, the X-ray diffraction analyses have shown a different behavior between these two substances with changing temperature. In case of $(NMe_4)_2TCNQ_3$ the diminishing of the S1 band arises from the decreasing of the slip distance as the temperature increases, which is indicated by the diminishing of the intensity of the Bragg reflection[20]. However, similar measurement on present substance shows that the slipped distance is almost unchanged by the changing temperature[21]. Therefore, the origin of the temperature dependence of S1 band in the present substance should be considered different from that of $(NMe_4)_2TCNQ_3$.

It is important to notice that the temperature dependence of the integrated intensity of S1 as well as the EMV band in the 0 and 5 T crystals resembles very much with the temperature dependence of the magnetization shown in Fig.4. If we draw the same curves as the magnetization with their baselines adjusted, they fit the experimental data of S1 band and EMV modes very well, as shown by the solid lines in Fig.7. These facts suggest that S1 as well as EMV bands are strongly linked to the magnetic properties of this substance.

As mentioned in the preceding section, the conductance data suggest the existence of acceptors with density of 10^{17} cm^{-3} in 0 T crystals. The band-to-bound absorption bands inside the gap mentioned in the preceding section, therefore, can be assigned to the electronic transition from the valence band to the acceptor levels, as well as from the acceptor levels to the conduction band. It is important to once again note that the bound-to-band absorption can only be observed if the probe light is polarized in the direction of TCNQ molecular stack, i. e. in E//b polarization. This fact indicates that these acceptors do not arise from normal type impurities, but rather incorporated in the TCNQ columns. We suggest that these acceptors arise from the disorder in the molecular arrangement in TCNQ columns.

The acceptor concentration in 5 T crystals, on the other hand, is found to be higher than that of 0 T crystals, as understood from electrical conductance measurement. It is noteworthy that the temperature dependence of electrical conductance of 5 T crystals compared to that of 0 T crystals resembles to the of the electrical conductivity of the disordered $NMe3.5MePy(TCNQ)_2$ after electron irradiation[22]. This suggests, therefore, that the applied field during the crystal growth has enhanced the disorder in the arrangement of TCNQ molecules along the column. Although not very straightly, the change in the band-to-bound absorption bands can be considered to be related to is enhancement.

The molecules at the disorder sites act as donors and acceptors, and in term of energy band they appear as the new levels in the gap. These levels renormalized the entire of the electronic structure, including the spin state, and drive the ferromagnetic behavior. In term of Dzyaloshinsky-Moriya interaction those disorder might result in the disappearance of the aforementioned inversion center. In 5 T crystals, where the disorder is enhanced, it is suggested that in the gap there appears some new energy levels induced by the applied filed. This results in the increasing of the Curie temperature as well as the intensifying of S1 and EMV bands.

It is important to notice that the threshold of the magnetic field is reduced if the growth temperature is lowered. At high temperature, the movement of the molecules due to the thermodinamical

forces might stronger than that due to the Lorentz force. As the result, a stronger field is necessary to gain the expected effects. When the temperature is lowered, the thermodynamical forces are getting weaker, which causes the Lorentz force to be more dominant, so that the field effects can be obtained at lower field strength.

In addition the case of NMe3.5MePy(TCNQ)$_2$ mentioned above, remarkable changes in the properties of organic substances due to the slight disorder in its structure have been studied by several authors. TTTF-TCNQ, for example, exhibits significant decrement of the conductivity maximum, and at the same time the increment of the Peierls transition temperature TP due to the disorder introduced by deuteron irradiation[23]. Magnetic properties are also very sensitive to such disorder. Miljak *et al.*[24] have shown that the low temperature susceptibility in TTF-TCNQ follow Curie law before irradiation to change to a $T^{0.74}$ dependence after the introduction of about 1% of paramagnetic defects by neutron bombardment. To the best of author's knowledge, the application of magnetic field as the method of introducing disorder has never been reported previously.

Recently, novel ferromagnetism with extremely small saturation magnetization but with Curie temperature higher than room temperature has also been observed in $Ca_{1-x}La_xB_6$[22], CaC_2B_2[23], and C_{60} polymer[24]. Similar to Cs_2TCNQ_3, these inorganic compounds do not contain magnetic metal elements, so that their ferromagnetism is beyond the known theory. Their saturation moment and Curie temperature are shown in Table 1. All of them have saturation moment of $10^{-3} - 10^{-4}$ μ_B/formula unit. In Cs_2TCNQ_3, as previously mentioned, there exist acceptors with density of 10^{17} cm^{-3}. Interestingly, if we convert this value in term of molecular unit, we will get 10^{-4}. This fact has been previously suggested from the electric conductance measurement results, but too premature to be connected to the magnetic properties. The optical data from the present work directly clarify that relation.

The results of the high-pressure infrared absorption measurement described in the preceding section clearly show the significant differences in the high-pressure properties of the crystals grown with and without magnetic field. The behavior of the C-CN as well as the C-H stretching indicates that phase transitions with properties similar to each other take place in both crystals. In 0 T crystals this phase transition has been shown to be strongly related to an insulator-metal transition[15-17], whereas this particular relation yet to be studied in 5 T crystals. The major difference lies on the fact that this phase transition in 5 T crystals takes place at around 4.2 GPa, whereas in 0 T crystals this transition takes place at 3.6 GPa.

The properties of this phase transition that occurs at in 0 T crystals have been discussed previously. In general, the phase transition observed at 4.2 GPa in 5 T crystals is very similar to this transition, except that it takes place at higher pressure. The delocalization of π^* electrons seems to take place

Table 1.

Substance	Tc (K)	Magnetic moment (μB/formula unit)
Cs_2TCNQ_3 (0 T crystal)	300	2×10^{-5}
Cs_2TCNQ_3 (5 T crystal)	400	2×10^{-3}
$Ca_{1-x}La_xB_6$	600	3×10^{-4}
CaC_2B_2	770	3.8×10^{-4}
Rh$-C_{60}$	500	6×10^{-4}

in 5 T crystals as well, as indicated by the abrupt decreasing of the frequency spacing between the vibration modes belonging to neutral and radical, particularly of the C-H stretching modes. The delocalization, however, is not high. The degree of the charge transfer estimated from the frequency of the C-H stretching modes at 5.3 GPa are $\rho = 0.30-0.37$ and $0.81-0.85$ for neutral and radical molecules, respectively. These values are significantly different from that of 0 T crystals, which give the values of $\rho = 0.46-0.50$ and $0.75-0.77$, respectively[17].

The EMV modes are originally forbidden in $E//a$ polarization, where E and a are the electric field of light and a-axis of the monoclinic crystal structure. They normally appear in the $E//b$ polarization, the stacking axis of the TCNQ molecules. In the present substance, however, they are also observable in $E//a$ polarization. This is because the $TCNQ^-$ molecules are stacked in a way that they are displaced against each other along the short molecular axis, i. e. a-axis, to form slipped dimers[7]. Because of this slip, the dipole moment of the inter-radical electronic transition is not perfectly parallel to b axis, but is slightly canted and has a small component along a axis. This component couples with the molecular vibration to drive the EMV modes, which appear along the $E//a$ polarization with much smaller intensity compared to the modes appear in E//b polarization. We have previously observed in the case of $(NMe_4)_2TCNQ_3$, which crystal structure is very similar to the present substance, that these modes disappear when the $TCNQ^-$ dimers are no longer slipped due to the phase transition[18-20]. The intensity of the EMV modes appear in E//a polarization, therefore, represents the amount of slip distance of the $TCNQ^-$ dimers.

We have previously shown that the EMV modes observed in the unpolarized spectrum in this substance reflects the properties of that observed in the $E//a$ polarization of the linearly polarized spectrum[17]. We have, therefore, suggested that the disappearance of this mode in the high-pressure phase of 0 T crystals is as the result of the change in relative position of the TCNQ molecules, and the slipped $TCNQ^-$ dimers turn into perfectly eclipsed ones, similar to the case of $(NMe_4)_2TCNQ_3$ mentioned above. The differences in the behavior of EMV band in respective crystals suggest that the relative positions of the TCNQ molecules in 5 T crystals might have been changed by the field. The changes, however, seem to be too microscopic to be detectable by the X-ray diffraction.

In the perspective of the crystal growth mechanism explained above, the disorders induced by the field manifest themselves as the changes in the relative positions of the TCNQ molecules. The new relative positions in the 5 T crystals result in additional forces that prevent the system from entering the delocalization state with the same degree as the 0 T crystals in the high-pressure phase.

Conclusion

The experimental results explained have shown that crystal growth under magnetic field is a very useful tool, not only for modifying the electronic structure, and therefore the properties, of the Cs_2TCNQ_3, but also provides valuable information for understanding the novel magnetic properties in this substance. The disorder in the molecular arrangement of the TCNQ has been found to play important role in driving the magnetic properties of this substance. Although the existence of these disorders have been suggested from the previous electrical conductivity measurements, its link to the magnetic properties has never been explored. This link would be hard to found without comparing the optical, electric, and magnetic properties of the 0 T and 5 T crystals. The disorder seems to be

strongly related to the relative position of the TCNQ molecules.

References

1. J. Torbet, J. M. Freyssinet and G. Hudry-Clergeon, Nature 289, 91 (1981).
2. Yamagishi, T. Takeuchi, T. Higashi and M. Date, J. Phys. Soc. Jpn. 58, 2280 (1989).
3. S. Yanagiya, J. Crystal Growth 196, 319 (1999).
4. Katsuki, R. Tokunaga, S. Watanabe and Y. Tanimoto, Chem. Lett. 607 (1996).
5. Y. Ma, K. Watanabe, S. Awaji, M. Motokawa, Appl. Phys. Lett. 77, 3633 (2000). See also the references therein.
6. K. Ueda, T. Sugimoto, S. Endo, N. Toyota, M. Kohama, K. Yamamoto, Y. Suenaga, H. Morimoto, T. Yamaguchi, M. Munakata, N. Hosoito, N. Kanehisa, Y. Shibamoto, Y. Kai, Chem. Phys. Lett. 261, 295 (1996).
7. C.J. Fritchie, Jr., P. Arthur, Jr., Acta Cryst. 21, 139 (1966).
8. A. Painelli, C. Pecile and A. Girland, Mol. Cryst. Liq. Cryst. 134, 1 (1986).
9. K. D. Cummings, D. B. Tanner, J. S. Miller, Phys. Rev. B 24, 4142 (1981).
10. Z. G. Soos and D. J. Klein, J. Chem. Phys. 55, 3284 (1971).
11. R. G. Kepler, J. Chem. Phys. 39, 3528 (1963).
12. J. S. Blakemore, J. E. Lane, D. A. Woodbury, Phys. Rev. 18, 6797 (1978).
13. J. Tanaka, M. Tanaka, T. Kawai, T. Takabe and O. Maki, Bull. Chem. Soc. Jpn. 49, 2358 (1976).
14. K. Yakushi, M. Iguchi, G. Katagiri, T. Kusaka, T. Ohta, H. Kuroda, Bull. Chem. Soc. Jpn., 54, 348 (1981).
15. S. Matsuzaki, Synth. Met. **61** (1993) 207.
16. Hasanudin, N. Kuroda, T. Kagayama, J. Phys. Condens. Matter. **14** (2002) 10419.
17. Hasanudin, N. Kuroda, T. Kagayama, T. Sugimoto, J. of Phy. Soc. Jpn., **72** (2003) 1784.
18. Hasanudin, N. Kuroda, T. Sugimoto, Synth. Met. 120 (2001) 1045.
19. N. Kuroda, Hasanudin, T. Sugimoto, K. Ueda, M. Kohama, N. Toyota, Synth. Met. 103 (1999) 2327.
20. K. Yagi, H. Terauchi, N. Kuroda, K. Ueda, T. Sugimoto, J. Phys. Soc. Jpn. 68 (1999) 3770.
21. K. Yagi, private communication.
22. M. Przybylski, W. Pukacki, L. Zupirolli, J. de Physique C3 (1983) 1369.
23. C. K. Chiang, M. J. Cohen, P. R. Newman, A. J. Heeger, Phys. Rev. B. 16 (1977) 5163.
24. M. Miljak, B. Korin, J. R. Cooper, K. Holcer, A. Janossy, J. Phys. 41 (1980) 639.
25. D. P. Young, D. Hall, M. E. Torelli, Z. Fisk, J. L. Sarrao, J. D. Thompson, H. -R. Ott, S. B. Oseroff, R. G. Goodrich and R. Zysler, Nature 397, 412 (1999).
26. J. Akimitsu, K. Takenawa, K. suzuki, H. Harima and Y. Kuramoto, Science 293, 1127 (2001).
27. T. N. Makarova, B. Sandqvist, R. Hohne, P. Esquinazi, Y. Kopelevich, P. Scharff, V. A. Davydov, L. S. Kashevarova and A. V. Rakhmanina, Nature 413, 716 (2001).